Supporting Information

Achieving Efficient Blue Room-Temperature Phosphorescence in Cyclized Aromatic Amides via Hybridized Local and Charge-Transfer State

Qiao He, Jia-Dong Guo, Ke Zhang, Yu-Zhe Chen,* Chen-Ho Tung and Li-Zhu Wu*

New Cornerstone Science Laboratory, CAS-HKU Joint Laboratory on New Materials, Technical Institute of Physics and Chemistry, Chinese Academy of Sciences, Beijing 100190, P. R. China; School of Future Technology, University of Chinese Academy of Sciences, Beijing 100049, P. R. China

E-mail: chenyuzhe@mail.ipc.ac.cn; lzwu@mail.ipc.ac.cn

Materials and methods

Unless otherwise noted, materials obtained from commercial suppliers were used without further purification. All NMR spectra were recorded on a Bruker 400 Hz in DMSO-d_6 or $CDCl_3$. NMR chemical shifts are reported in ppm referenced to the solvent peaks of $CDCl_3$ (7.26 ppm for ^1H and 77.16 ppm for ^{13}C, respectively) or DMSO-d_6 (2.50 ppm for ^1H and 39.50 ppm for ^{13}C, respectively). High-resolution mass spectrometry experiments were performed with a Bruker Apex IV Fourier Transform High Resolution Mass Spectrometer. Absorption spectra were recorded on a Hitachi U-3900 UV-visible spectrophotometer. Photoluminescence spectra were measured on a Horiba Fluoremax-4 PLUS spectrofluorometer (HORIBA Instruments Incorporated, Edison, USA) with a xenon lamp as an excitation light source. Luminescence decays were measured by time-correlated single photon counting technique using a FLS920 Edinburgh spectrometer with a microsecond flash lamp (μF 900), Xe lamp or pulsed laser. The values of lifetime were calculated by exponential function fitting with luminescence spectrometer software F900. Absolute quantum yields were measured by using a FLS1000 Edinburgh spectrometer with an integrated sphere. Single crystal X-ray diffraction data were collected on CrysAlisPro 1.171.42.72a (Rigaku Oxford Diffraction, 2022).

General Procedure for Synthesis

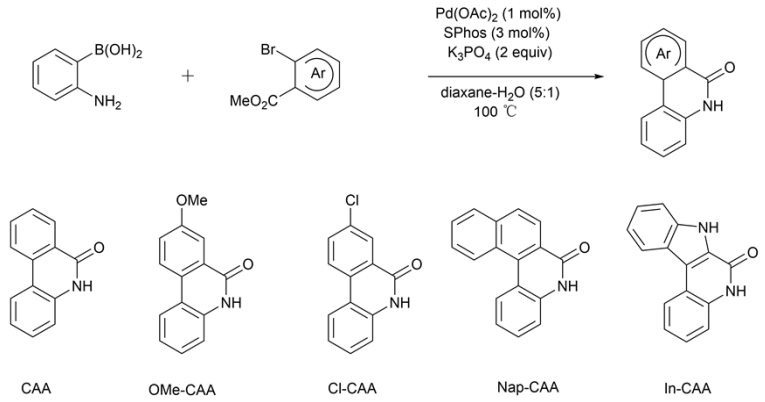

Fig. S1 The synthetic route of CAA and its derivatives

CAA and its derivatives were synthesized based on the reported works.[1, 2]

CAA: A pressure-resistant tube, which was equipped with a magnetic stir bar and fitted with a teflon septum, was charged with $Pd(OAc)_2$ (1 mol%), 2-dicyclohexylphosphino-2',6'-dimethoxybiphenyl (SPhos) (3 mol%), 1,4-dioxane (1 mL) and H_2O (1 drop) under argon environment. The resulting solution was stirred for 20 min. A round bottom flask was charged with methyl 2-bromobenzoate (0.580 mmol, 1 equiv.), 2-aminophenylboronic acid (0.703 mmol, 1.2 equiv.), K_3PO_4 (1.154 mmol, 2 equiv.), 1,4-dioxane (1 mL) and H_2O (1 drop). The

mixture was transferred into the first reaction vessel, then additional 1,4-dioxane (3 mL) was added in argon environment. The vessel was sealed with a screw cap, and the solution was heated at 100 °C for 24 h. After completion of reaction, reaction mixture was poured over water, extracted with ethyl acetate, dried over Na_2SO_4, and evaporated under vacuum on rotary evaporator. Obtained product was purified by column chromatography on silica gel using n-Hexane/EtOAc (2:1). Then the resulting white solid was dissolved in dichloromethane and slowly recrystallized with *n*-hexane to afford white needle shaped crystal; ^{1}H NMR (400 MHz, DMSO-d_6, δ): 11.69 (s, 1H), 8.55 - 8.48 (m, 1H), 8.40 (dd, J = 8.2, 1.4 Hz, 1H), 8.34 (dd, J = 8.0, 1.5 Hz, 1H), 7.86 (ddd, J = 8.4, 7.2, 1.5 Hz, 1H), 7.66 (ddd, J = 8.1, 7.1, 1.1 Hz, 1H), 7.50 (ddd, J = 8.3, 7.1, 1.3 Hz, 1H), 7.38 (dd, J = 8.2, 1.3 Hz, 1H), 7.27 (ddd, J = 8.2, 7.1, 1.3 Hz, 1H); ^{13}C NMR (101 MHz, DMSO-d_6, δ): 160.8, 136.5, 134.2, 132.8, 129.5, 127.9, 127.4, 125.7, 123.2, 122.6, 122.2, 117.5, 116.1; HRMS (ESI) m/z $[M+H]^+$ calcd for $C_{13}H_9NO$, 196.0762; found, 196.0760.

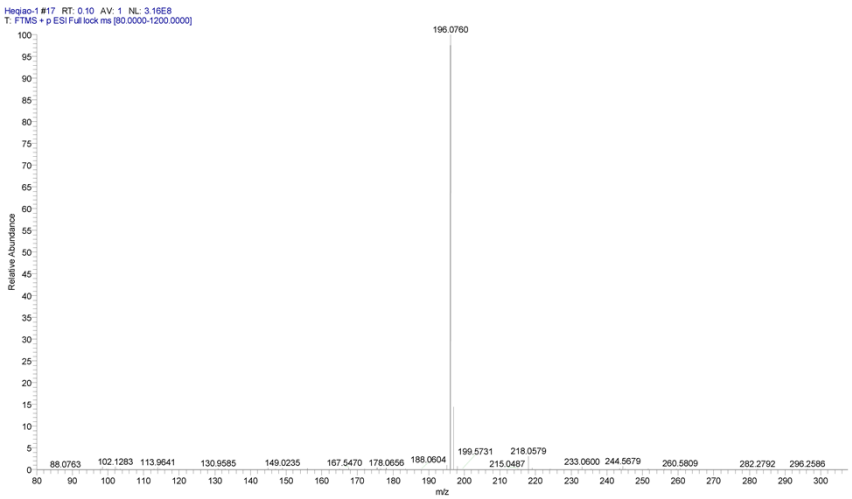

Fig. S2 HR-ESI-MS of CAA

OMe-CAA: White solid; ^{1}H NMR (400 MHz, DMSO-d_6, δ): 11.70 (s, 1H), 8.44 (d, J = 9.0 Hz, 1H), 8.30 (dd, J = 8.2, 1.3 Hz, 1H), 7.76 (d, J = 2.8 Hz, 1H), 7.47 - 7.43 (m, 1H), 7.43 - 7.40 (m, 1H), 7.34 (dd, J = 8.1, 1.4 Hz, 1H), 7.24 (ddd, J = 8.2, 7.1, 1.4 Hz, 1H), 3.91 (s, 3H); ^{13}C NMR (101 MHz, DMSO-d_6, δ): 160.5, 159.0, 135.5, 128.4, 127.6, 127.1, 124.6, 122.6, 122.3, 121.6, 117.7, 115.9, 108.7, 55.4; HRMS (ESI) m/z $[M+H]^+$ calcd for $C_{14}H_{11}NO_2$, 226.0868; found, 226.0863.

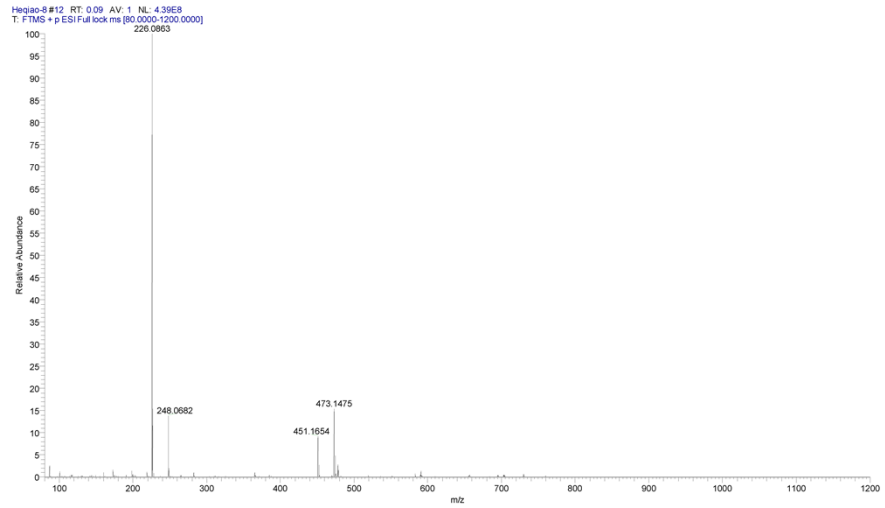

Fig. S3 HR-ESI-MS of OMe-CAA

Cl-CAA: White solid; ^{1}H NMR (400 MHz, DMSO-d_6, δ): 11.81 (s, 1H), 8.51 (d, J = 8.7 Hz, 1H), 8.37 - 8.31 (m, 1H), 8.21 (d, J = 2.4 Hz, 1H), 7.85 (dd, J = 8.7, 2.2 Hz, 1H), 7.48 (t, J = 7.6 Hz, 1H), 7.35 (d, J = 8.0 Hz, 1H), 7.25 (t, J = 7.3 Hz, 1H); ^{13}C NMR (101 MHz, DMSO-d_6, δ): 159.7, 136.5, 133.1, 132.8, 132.7, 130.0, 127.2, 126.6, 125.2, 123.4, 122.5, 116.9, 116.2; HRMS (ESI) m/z $[M+H]^+$ calcd for $C_{13}H_8ClNO$, 230.0372; found, 230.0369.

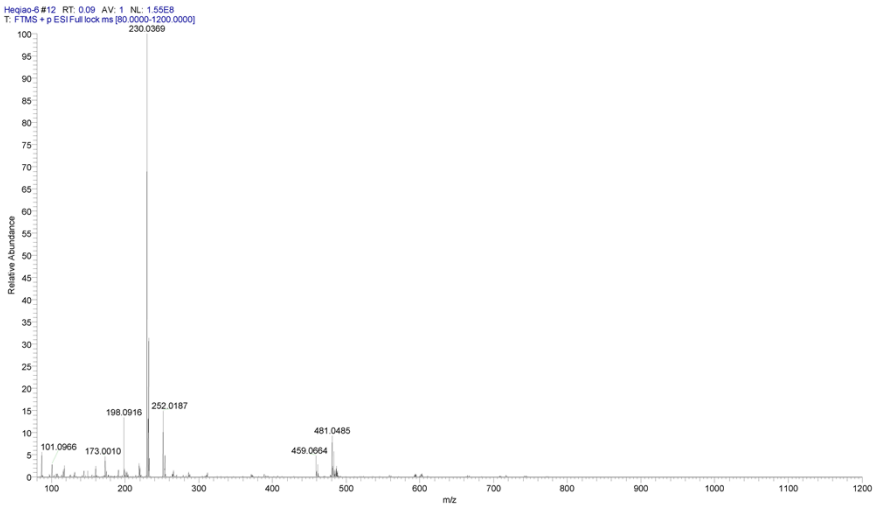

Fig. S4 HR-ESI-MS of Cl-CAA

In-CAA: White solid; ^{1}H NMR (400 MHz, DMSO-d_6, δ): 12.37 (s, 1H), 11.88 (s, 1H), 8.52 – 8.42 (m, 2H), 7.66 (d, J = 8.2 Hz, 1H), 7.53 (dd, J = 8.1, 1.3 Hz, 1H), 7.49 (ddd, J = 8.2, 7.0, 1.0 Hz, 1H), 7.42 (td, J = 8.2, 7.7, 1.4 Hz, 1H), 7.40 – 7.29 (m, 2H); ^{13}C NMR (101 MHz, DMSO-d_6, δ): 155.7, 138.8, 135.0, 127.6, 125.9, 125.7, 123.0, 122.3, 122.3, 122.3, 120.7, 118.2, 118.0, 116.1, 113.1; HRMS (ESI) m/z $[M+H]^+$ calcd for $C_{15}H_{10}N_2O$, 235.0871; found, 235.0866.

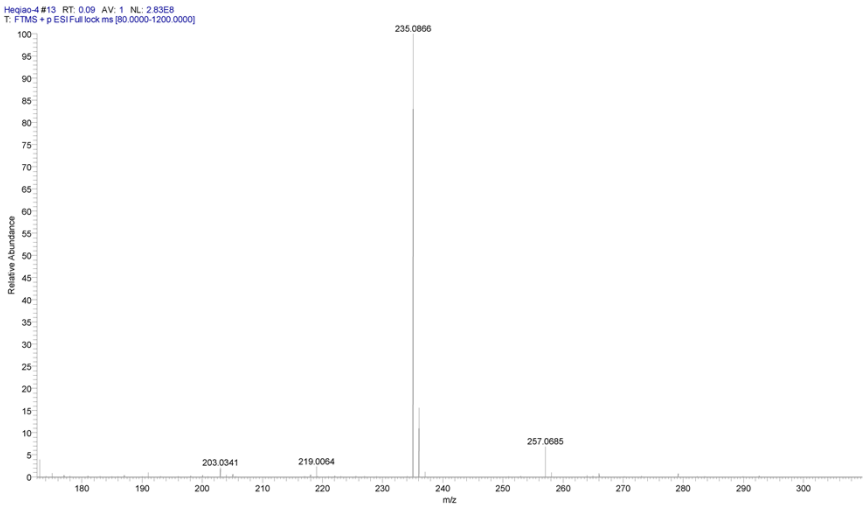

Fig. S5 HR-ESI-MS of In-CAA

Nap-CAA: White solid; ^{1}H NMR (400 MHz, DMSO-d_6, δ): 11.95 (s, 1H), 8.98 - 8.90 (m, 1H), 8.64 - 8.57 (m, 1H), 8.32 (d, J = 8.6 Hz, 1H), 8.18 - 8.12 (m, 1H), 8.09 (d, J = 8.6 Hz, 1H), 7.80 - 7.74 (m, 2H), 7.56 (ddd, J = 8.2, 6.9, 1.3 Hz, 1H), 7.51 (dd, J = 8.2, 1.6 Hz, 1H), 7.34 (ddd, J = 8.4, 6.9, 1.6 Hz, 1H); ^{13}C NMR (101 MHz, DMSO-d_6, δ): 160.8, 137.3, 135.7, 132.8, 129.24, 128.9, 128.5, 128.3, 128.1, 127.8, 127.3, 127.3, 124.5, 122.8, 122.0, 117.4, 116.3; HRMS (ESI) m/z $[M+H]^+$ calcd for $C_{17}H_{11}NO$, 246.0919; found, 246.0914.

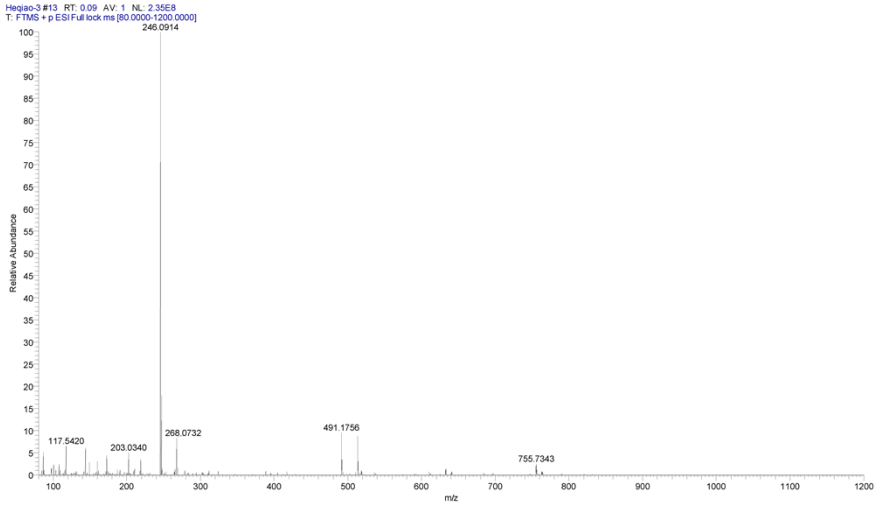

Fig. S6 HR-ESI-MS of Nap-CAA

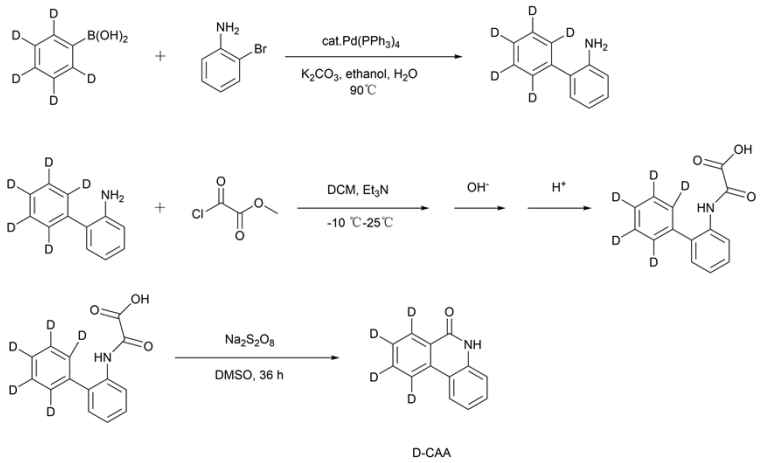

Fig. S7 The synthetic route of D-CAA

D-CAA was synthesized based on the reported works.[3]

D-CAA: White solid; ^{1}H NMR (400 MHz, DMSO-d_6, δ): 11.68 (s, 1H), 8.43 - 8.36 (m, 1H), 7.50 (ddd, J = 8.3, 7.1, 1.4 Hz, 1H), 7.37 (ddd, J = 8.2, 1.3, 0.5 Hz, 1H), 7.27 (ddd, J = 8.3, 7.1, 1.3 Hz, 1H); ^{13}C NMR (101 MHz, DMSO-d_6, δ): 161.2, 137.0, 134.6, 130.0, 126.0, 123.7, 122.7, 118.0, 116.5; HRMS (ESI) m/z $[M+H]^+$ calcd for $C_{13}D_4H_5NO$, 200.1013; found, 200.1009.

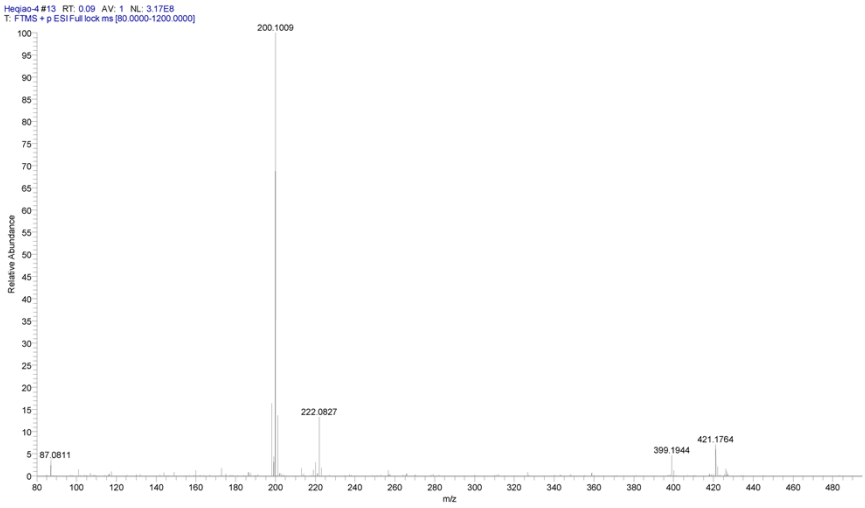

Fig. S8 HR-ESI-MS of D-CAA

AA: Benzanilide (AA) is commercially available from Macklin (98%) and was used after recrystallization from dichloromethane and *n*-hexane as white crystals. ^{1}H NMR (400 MHz, Chloroform-*d*, δ): 7.90 - 7.84 (m, 3H), 7.65 (d, J = 7.6 Hz, 2H), 7.59 - 7.52 (m, 1H), 7.51 - 7.44 (m, 2H), 7.41 - 7.33 (m, 2H), 7.19 - 7.12 (m, 1H); ^{13}C NMR (101 MHz, Chloroform-*d*, δ): 165.8, 137.9, 135.0, 131.8, 129.1, 128.8, 127.0, 124.6, 120.2; HRMS (ESI) m/z $[M+H]^+$ calcd for $C_{13}H_{11}NO$, 198.0919; found, 198.0917.

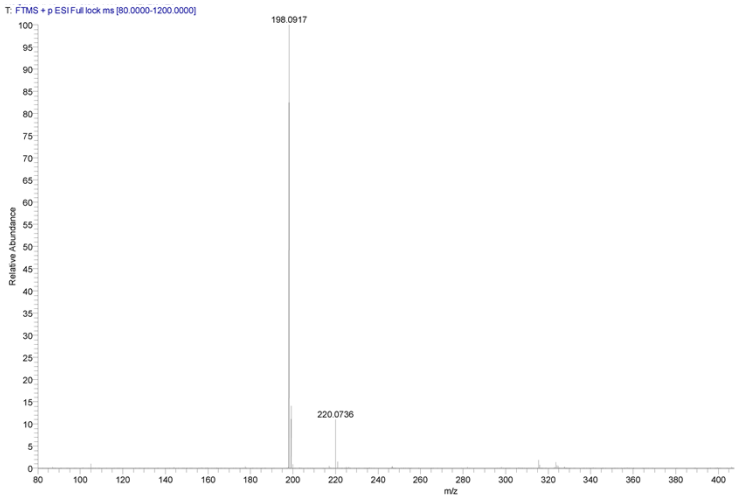

Fig. S9 HR-ESI-MS of AA

Preparation of hybrid films

PVA (3.0 g) was dissolved in deionized water (300 mL) and heated to 95 °C for 6 hours to obtain PVA aqueous solution (10.0 mg/mL) for further use. THF solution of the corresponding compounds were added into certain amount of the PVA solution. Take CAA@PVA100 as an example, 0.5 mL THF solution of CAA (0.3 mg/mL) was added into 10 mL of the PVA aqueous solution. The resulting mixtures were ultrasonicated for 1 hour for dissolution. The aqueous solution was then drop-coated on quartz glass and evaporated under vacuum to get uniform and transparent films. It should be noted that the prepared films need to be stored in a water-free environment.

Photophysical properties investigation

Table S1. Photophysical properties of AA, CAA and its derivatives.

Sample	λ_{abs} (ε)	Solution		77 K					PVA					
	[nm][a]	λ_f [nm][a]	Φ_f [%][a]	λ_f [nm][b]	τ_f [ns][b])	λ_p [nm(eV)][b]	τ_p [ms][b]	Φ_{PL} [%][c]	λ_f [nm][c]	τ_f [ns][c]	Φ_f [%][c]	λ_p [nm(eV)][c]	τ_p [ms][c]	Φ_p [%][c]
CAA	321 (10,000)	361	12.9	359	1.1	424(2.93)	3287.2	25.6	361	0.4	10.0	425(2.92)	2016.9	15.6
D-CAA	321 (9,300)	361	12.8	358	1.3	424(2.93)	3751.5	12.6	361	0.9	3.9	425(2.92)	2230.4	8.7
OMe-CAA	311 (10,800)	371	16.5	367	1.2	434(2.86)	2432.5	18.2	378	0.7	11.1	437(2.84)	1572.4	7.1
Cl-CAA	327 (12,600)	376	7.0	369	0.9	435(2.85)	663.5	10.7	388	0.8	4.0	439(2.83)	293.7	6.6
In-CAA	345 (22,100)	368	44.4	370	1.7	469(2.64)	1489.4	18.5	378	2.1	15.9	484(2.56)	1156.7	2.6
Nap-CAA	327 (14,100)	400	20.0	400	1.5	521(2.38)	526.1	19.9	416	1.9	17.3	520(2.38)	344.2	2.6
AA	263 (31,100)	304	2.7	298	1.0	418(2.97)	271.1	7.1	-	-	-	456(2.72)	29.6	7.1

In either case, the excitation wavelength (λ_{ex}) of CAA and its derivatives is 300 nm, while λ_{ex} of AA is 250 nm. [a] In acetonitrile solution at room temperature (C = 1.0×10^{-5} M); [b] In 2-MTHF at 77 K (C = 1.0×10^{-5} M); c In PVA matrix at 0.3% mass ratio under ambient condition.

Table S2. The key examples of organic blue RTP systems in recent years.

References	τ_P (s)	Φ_P (%)
Angew. Chem. Int. Ed., 2024, **63**, e202403773.	1.9	14.4
Angew. Chem. Int. Ed., 2021, **60**, 17094-17101.	5.1	16.1
Nat. Mater., 2021, **20**, 1539-1544.	0.2	96.5
J. Am. Chem. Soc., 2024, **147**, 1474.	2.2	42.6
Angew. Chem. Int. Ed., 2023, **62**, e202300927.	0.9	24.2
J. Mater. Chem. C, 2025, **13**, 12754-12761.	0.7	24.3
This work	2.0 (CAA) 29.6 ms (AA)	15.6 (CAA) 7.1 (AA)

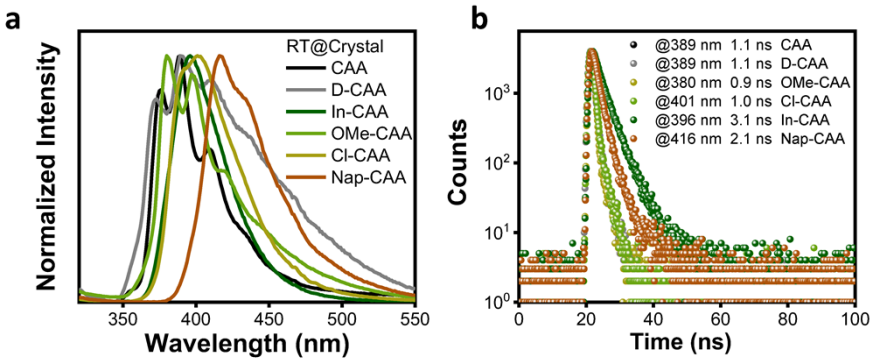

Fig. S10 Prompt emission spectra (a) and fluorescence decay profile (b) of CAA, D-CAA, OMe-CAA, Cl-CAA, In-CAA and Nap-CAA at crystal state.

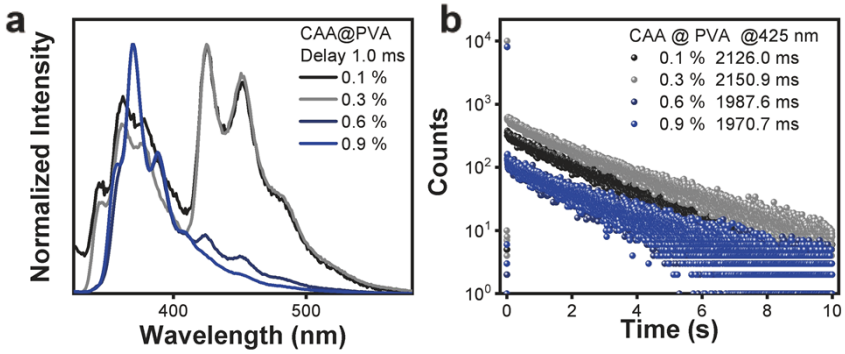

Fig. S11 (a) Prompt emission spectra and (b) time-resolved phosphorescence decay curves monitored at 425 nm of CAA@PVA at different doping ratios (λ_{ex} = 300 nm, delayed time = 1.0 ms).

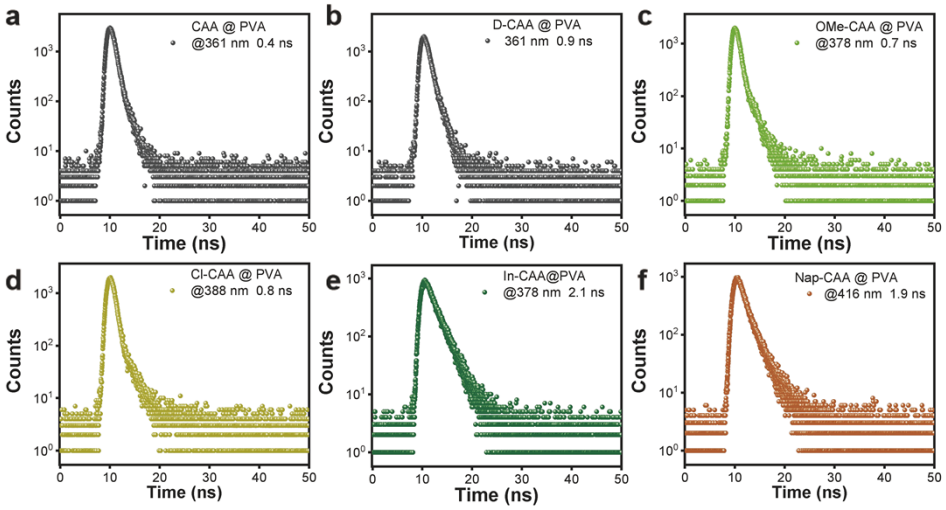

Fig. S12 Fluorescence decay profiles of CAA, D-CAA, OMe-CAA, Cl-CAA, In-CAA and Nap-CAA in PVA at a ratio of 0.3%.

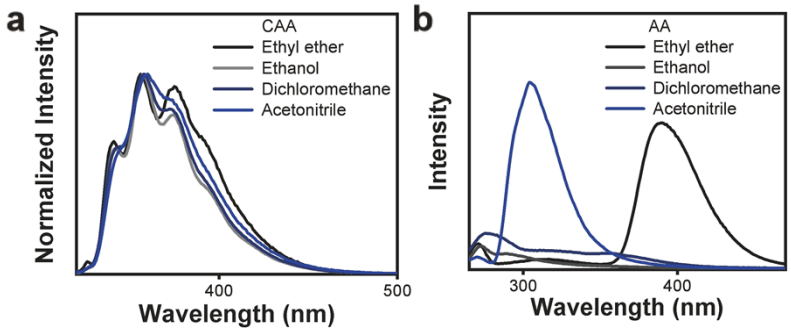

Fig. S13 Fluorescence spectra of CAA and AA in different solvents (C = 1.0×10^{-5} M, λ_{ex} = 300 nm).

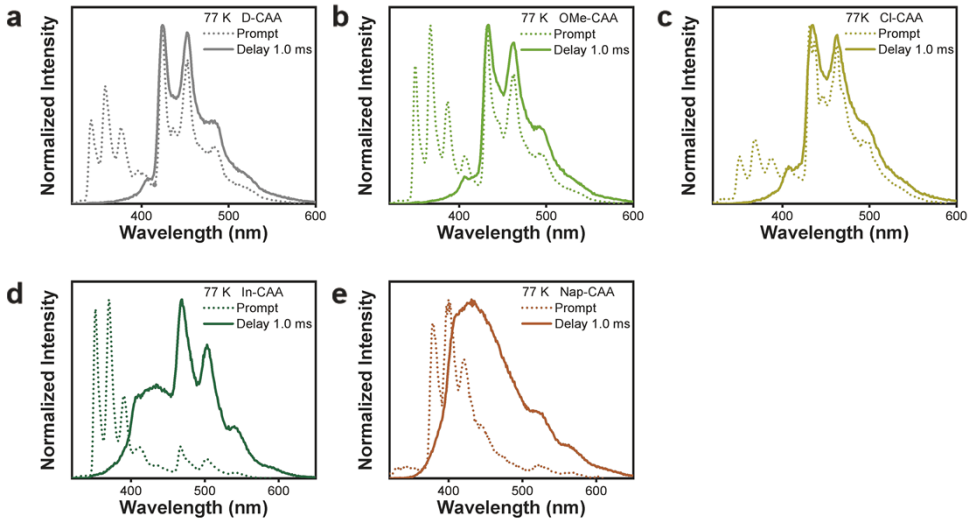

Fig. S14 Prompt and delayed emission spectra of D-CAA@2-MTHF, OMe-CAA@2-MTHF, Cl-CAA@2-MTHF, In-CAA@2-MTHF and Nap-CAA@2-MTHF (λ_{ex} = 300 nm, C=1.0×10^{-5} M).

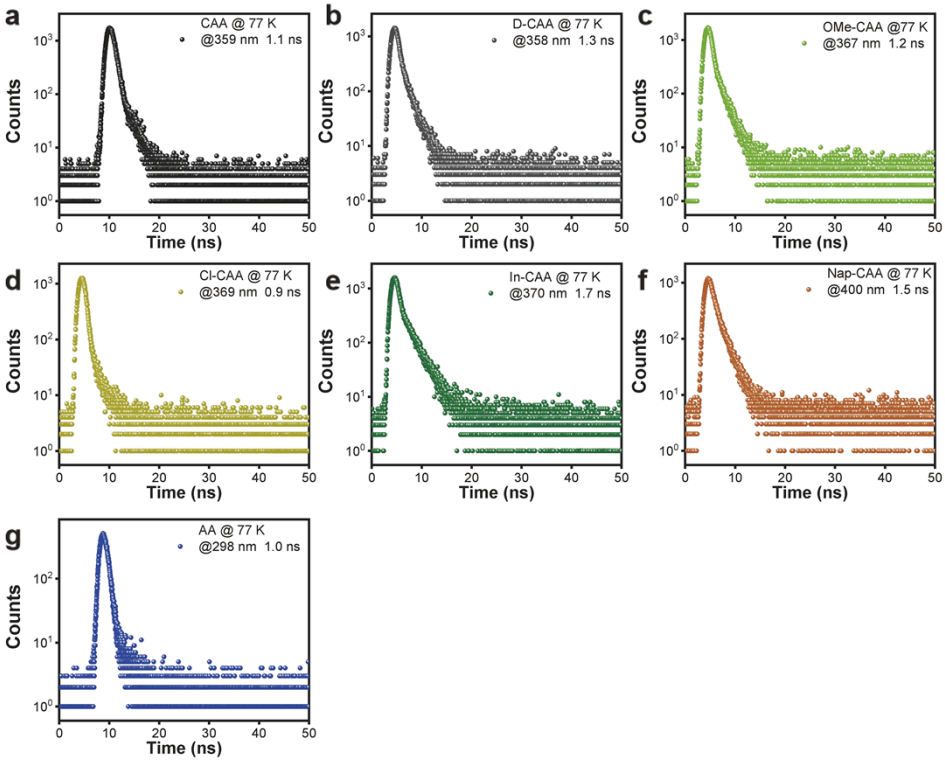

Fig. S15 Fluorescence decay profiles of CAA, D-CAA, OMe-CAA, Cl-CAA, In-CAA, Nap-CAA and AA in 2-MTHF at 77 K (C = 1.0×10^{-5} M).

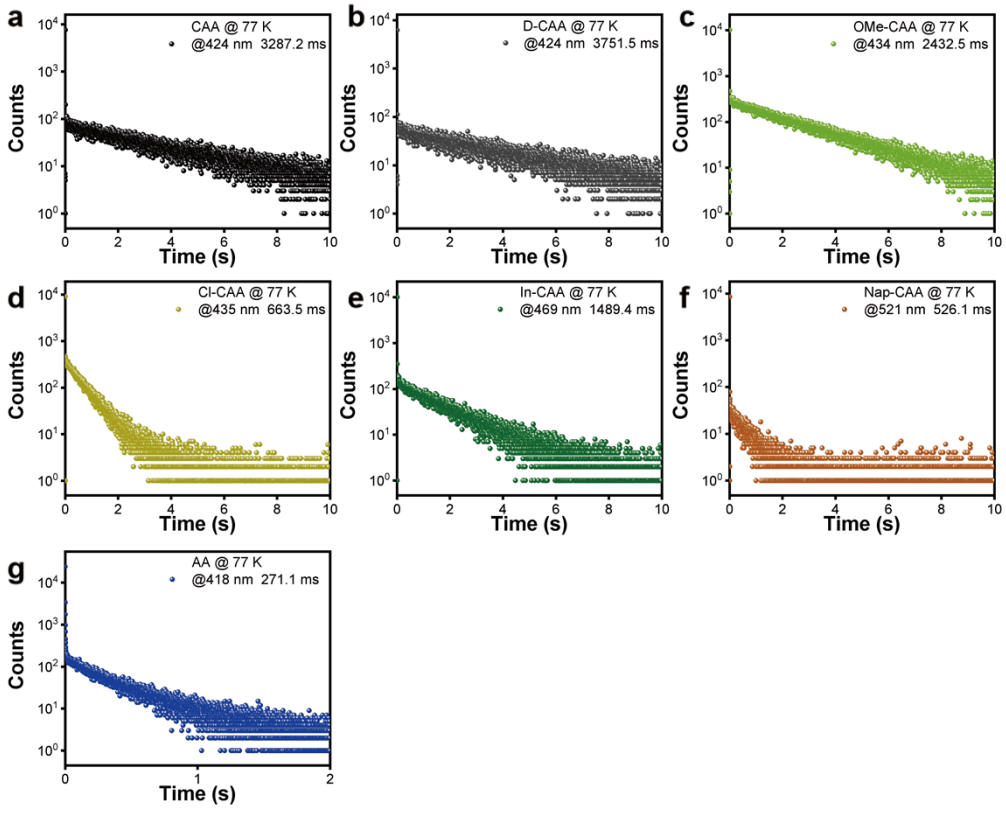

Fig. S16 Phosphorescence decay profiles of CAA, D-CAA, OMe-CAA, Cl-CAA, In-CAA, Nap-CAA and AA in 2-MTHF at 77 K (C = 1.0×10^{-5} M).

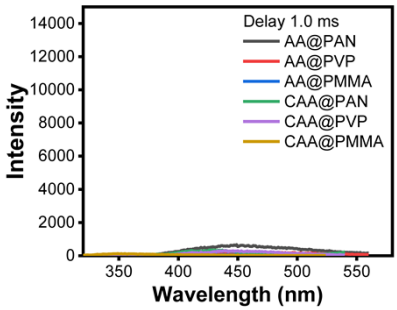

Fig. S17 The phosphorescence spectra of AA and CAA in different polymer matrices at a ratio of 0.3%.

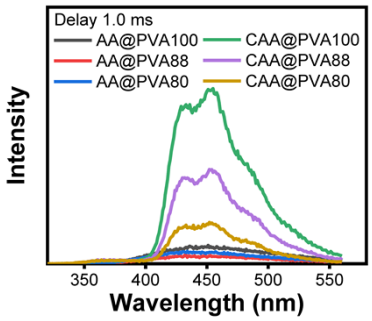

Fig. S18 The prompt and delayed spectra of AA and CAA in different alcoholysis degrees of PVA (PVA100, PVA88 and PVA80). CAA exhibits much stronger and sensitive RTP than that of AA in PVA with different alcoholysis degrees. This confirms that CAA might form stronger or more effective interactions with PVA compared to AA.

Theoretical details

These two molecules were optimized with dispersion corrected density functional theory (DFT-D3) at the PBE0-D3/def2-SVP level.[4, 5] The SMD (Solvation Model Based on Density)[6] implicit solvent model was used to describe the solvation effect of acetonitrile. In order to investigate the photophysical properties of these molecules, the excited electronic structures were calculated at the PBE0-D3/def2-SVP level with the time-dependent density functional theory (TDDFT) method. The spin-orbit coupling (SOC) matrix elements were calculated using the spin-orbit mean-field (SOME) methods based on the excited state wave functions obtained from TDDFT calculations. All these calculations were performed using ORCA 5.0.2 program.[7] The visualization of the frontier molecular orbitals were rendered using Visual Molecular Dynamic program (VMD).[8] The natural transition orbits (NTOs) and the contributions of

molecular orbital transitions were obtained by electron excitation analysis from the transition density matrix of TD-DFT calculation using Multiwfn program.

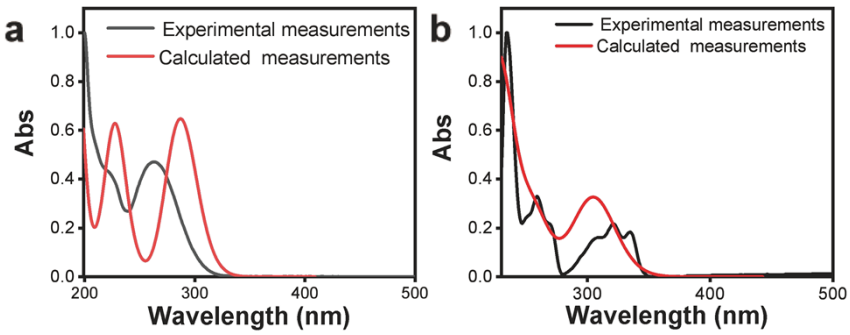

Fig. S19 The calculated and experimental absorption spectra of AA and CAA in acetonitrile.

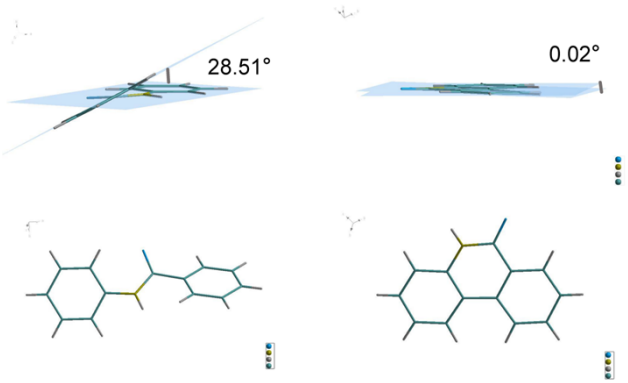

Fig. S20 The optimized S_0 geometry and dihedral angle of AA (left) and CAA (right).

Table S3. Theoretical calculation of excitation energies and corresponding wavelengths of AA.

	S		T	
	[eV]	[nm]	[eV]	[nm]
1	4.319	287.1	3.357	369.38
2	4.558	272.05	3.597	344.73
3	4.904	252.85	4.142	299.37
4	4.998	248.1	4.214	294.26
5	5.217	237.68	4.27	290.4
6	5.422	228.7	4.363	284.21
7	5.451	227.48	4.574	271.1
8	5.709	217.2	4.709	263.33
9	5.867	211.35	4.834	256.52
10	6.042	205.23	4.931	251.47
11	6.192	200.26	5.305	233.74
12	6.221	199.32	5.72	216.78
13	6.285	197.3	5.799	213.83
14	6.478	191.42	5.885	210.71
15	6.484	191.24	5.997	206.77

Table S4. Theoretical calculation of excitation energies and corresponding wavelengths of CAA.

	S		T	
	[eV]	[nm]	[eV]	[nm]
1	4.039	307.01	3.076	403.12
2	4.304	288.1	3.416	363
3	4.646	266.9	3.724	332.98
4	4.705	263.55	3.835	323.34
5	4.866	254.83	4.199	295.31
6	5.17	239.85	4.363	284.21
7	5.288	234.49	4.397	282.01
8	5.376	230.65	4.557	272.11
9	5.683	218.19	4.681	264.9
10	5.802	213.72	4.958	250.1
11	6.05	204.96	5.127	241.86
12	6.143	201.86	5.518	224.72
13	6.193	200.23	5.746	215.8
14	6.295	196.98	5.828	212.77
15	6.45	192.25	6.064	204.49

Table S5. The spin-orbit coupling (SOC) of AA.

cm^{-1}	S_0	S_1	S_2	S_3	S_4	S_5	S_6	S_7	S_8	S_9	S_{10}	S_{11}	S_{12}	S_{13}	S_{14}	S_{15}
T_1	1.3	0.7	10.7	0.2	1.6	0.1	0.5	1.1	0.3	0.1	0.3	0.5	3.3	2.4	0.7	1.0
T_2	6.8	4.5	12.1	0.8	1.4	0.3	2.1	4.1	2.0	1.2	0.5	0.3	0.8	0.2	0.3	0.6
T_3	21.6	8.8	9.4	1.6	2.0	0.5	3.7	8.0	6.5	0.8	2.5	0.4	3.3	1.3	2.0	2.3
T_4	23.4	6.3	10.0	0.5	0.7	0.3	2.8	6.8	5.5	0.6	6.8	0.2	0.8	1.0	0.4	1.5
T_5	11.8	2.8	9.3	0.1	0.8	0.2	1.3	3.2	3.3	1.1	7.2	0.2	0.7	1.0	1.6	0.3
T_6	10.8	3.6	1.1	0.6	0.3	0.6	1.6	3.6	3.4	1.5	0.2	0.6	0.5	1.6	0.5	0.6
T_7	8.3	0.9	10.5	0.1	0.8	1.4	0.3	1.1	1.3	2.6	0.4	0.4	0.4	0.9	0.5	0.9
T_8	1.8	1.1	8.6	0.2	0.8	0.3	0.4	0.6	0.4	1.6	0.6	0.8	5.2	4.0	0.7	1.4
T_9	0.7	0.3	0.2	0.1	0.1	0.1	0.5	0.3	0.1	0.7	3.4	0.5	1.7	1.3	0.1	0.8
T_{10}	1.2	0.8	0.8	0.0	0.3	2.8	0.1	0.2	0.7	3.0	0.3	0.5	0.5	1.7	0.1	0.3
T_{11}	1.3	0.3	0.9	0.1	2.8	1.9	0.8	1.9	4.7	17.7	1.2	3.6	4.3	4.8	0.3	1.2
T_{12}	1.3	2.5	25.7	1.5	3.0	0.1	0.9	1.7	1.3	0.8	1.8	1.0	7.9	6.6	1.3	3.2
T_{13}	1.0	0.1	1.0	0.5	0.3	0.9	0.6	0.3	1.2	0.3	2.0	0.6	1.2	1.8	0.1	1.0
T_{14}	3.3	0.2	0.4	0.5	3.2	15.9	0.6	1.2	2.2	5.5	0.4	3.2	4.4	8.6	0.7	0.9
T_{15}	4.1	1.1	1.8	8.9	0.4	0.6	8.6	1.5	0.7	0.1	0.9	1.0	0.4	0.3	5.3	0.9

Table S6. The spin-orbit coupling (SOC) of CAA.

cm^{-1}	S_0	S_1	S_2	S_3	S_4	S_5	S_6	S_7	S_8	S_9	S_{10}	S_{11}	S_{12}	S_{13}	S_{14}	S_{15}
T_1	0.0	0.0	0.0	0.0	7.8	0.0	7.2	0.0	0.0	0.0	0.0	0.0	2.6	0.0	0.0	0.0
T_2	0.1	0.0	0.0	0.0	20.6	0.0	1.0	0.0	0.0	0.0	0.0	0.0	4.2	0.0	0.0	0.0
T_3	0.0	0.0	0.0	0.0	5.9	0.1	9.3	0.1	0.0	0.0	0.0	0.0	2.6	0.0	0.0	0.0
T_4	0.0	0.0	0.0	0.0	8.4	0.0	8.8	0.0	0.0	0.0	0.0	0.0	4.0	0.0	0.0	0.0
T_5	0.0	0.0	0.0	0.0	8.0	0.0	0.6	0.0	0.0	0.0	0.0	0.0	11.4	0.0	0.0	0.0
T_6	37.0	10.3	10.3	3.7	0.2	9.1	0.0	4.0	8.3	10.8	10.0	1.1	0.1	1.4	0.2	6.4
T_7	0.0	0.0	0.0	0.0	9.0	0.0	9.5	0.0	0.0	0.0	0.0	0.0	3.1	0.0	0.0	0.0
T_8	0.0	0.0	0.0	0.0	8.4	0.0	7.7	0.0	0.0	0.1	0.0	0.0	4.0	0.0	0.0	0.0
T_9	0.0	0.0	0.0	0.0	1.0	0.0	6.4	0.0	0.0	0.0	0.0	0.0	4.3	0.0	0.0	0.0
T_{10}	0.1	0.0	0.0	0.0	2.7	0.0	6.7	0.0	0.0	0.0	0.0	0.0	3.2	0.0	0.0	0.0
T_{11}	9.7	14.0	14.1	4.2	0.3	3.8	0.1	8.8	3.9	11.9	1.9	7.3	0.0	2.7	1.8	7.3
T_{12}	0.0	0.0	0.0	0.0	5.9	0.0	4.0	0.0	0.0	0.0	0.0	0.0	2.7	0.0	0.0	0.0
T_{13}	0.1	0.0	0.0	0.0	10.6	0.0	6.6	0.0	0.0	0.0	0.0	0.0	5.3	0.0	0.0	0.0
T_{14}	0.0	0.0	0.0	0.0	19.1	0.0	0.9	0.0	0.0	0.0	0.0	0.0	11.7	0.0	0.0	0.0
T_{15}	13.7	0.4	4.3	5.0	0.7	7.2	0.2	11.6	5.9	0.4	9.7	0.5	0.1	0.0	15.2	7.6

Table S7. The natural transition orbits (NTOs) of AA and CAA.

Sample	Energy level	Hole	Electron	Transition
AA	S_1	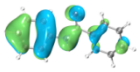	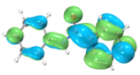	π→π*
	S_2	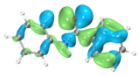	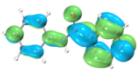	n→π*
	T_1	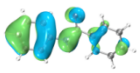	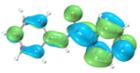	π→π*
	T_3	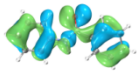	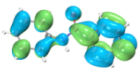	n→π*
	T_4	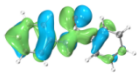	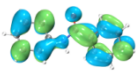	n→π*
		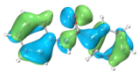	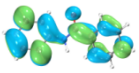	
	T_5	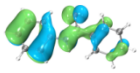	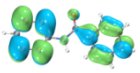	n→π*
	T_6	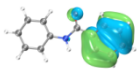	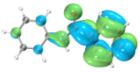	n→π*
	T_7	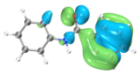	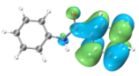	n→π*
		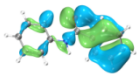	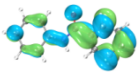	
CAA	S_1			π→π*
	S_2			π→π*
	T_1			π→π*
	T_6			n→π*

Table S8. Dynamic photophysical parameters of AA, CAA and its derivatives.

Sample	τ_f [ns]	τ_p [s]	Φ_f [%]	Φ_p [%]	$k_{f,r}$ [s^{-1}]	Φ_{isc} [%]	k_{isc} [s^{-1}]	$k_{p,r}$ [s^{-1}]	$k_{p,nr}$ [s^{-1}]
CAA	0.38	2.02	10.01	15.61	2.63×10^8	89.99	2.25×10^9	0.09	0.41
D-CAA	0.87	2.23	3.93	8.70	4.52×10^7	96.07	1.10×10^9	0.04	0.40
OMe-CAA	0.74	1.57	11.07	7.14	1.50×10^8	88.93	1.20×10^9	0.05	0.59
Cl-CAA	0.76	0.29	4.01	6.61	5.28×10^7	95.99	1.26×10^9	0.24	3.21
In-CAA	2.13	1.16	15.94	2.60	7.48×10^7	84.06	3.95×10^8	0.03	0.83
Nap-CAA	1.90	0.34	17.30	2.58	9.11×10^7	82.70	$4.\times10^8$	0.09	2.85
AA	-	0.03	0	7.10	-	100	-	2.37	30.96

The dynamic photophysical parameters were calculated based on following equations:

$$k_{f,r} = \Phi_f / \tau_f \quad (1)$$

$$\Phi_{isc} = 1-\Phi_f-\Phi_{ic} \approx 1-\Phi_f \quad (2)$$

$$\tau_f = 1/(k_{f,r}+ k_{f,nr}+ k_{isc});$$

$$\Phi_{isc} = k_{isc}/(k_{f,r}+ k_{f,nr}+ k_{isc}) = k_{isc} \times \tau_f;$$

$$k_{isc} = \Phi_{isc} / \tau_f \quad (3)$$

$$\tau_p = 1/(k_{p,r}+ k_{p,nr});$$

$$\Phi_p = (\Phi_{isc}\times k_{p,r})/(k_{p,r}+ k_{p,nr}) = \Phi_{isc}\times k_{p,r}\times\tau_p;$$

$$k_{p,r} = \Phi_p /(\Phi_{isc}\times\tau_p) \quad (4)$$

$$k_{p,nr} = 1/\tau_p-k_{p,r} \quad (5)$$

Where $k_{f,r}$, k_{isc} , $k_{p,r}$, $k_{p,nr}$ are the radiative rate constant of prompt fluorescence, rate constant of intersystem crossing (ISC), radiative rate constant of phosphorescence, and nonradiative rate constant of phosphorescence.

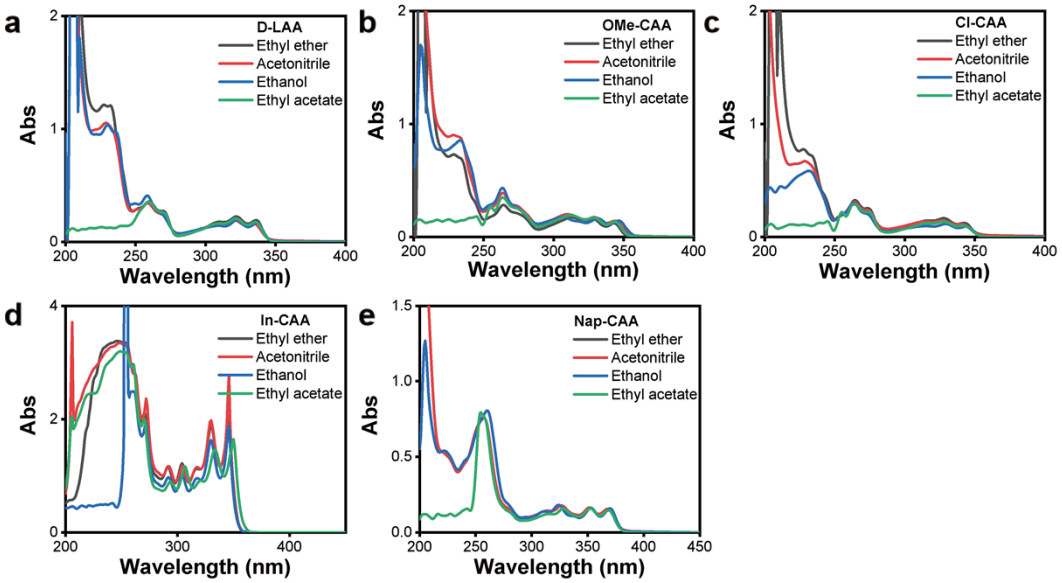

Fig. S21 Absorption spectra of D-CAA, OMe-CAA, Cl-CAA, In-CAA and Nap-CAA (C = 1.0×10^{-5} M, λ_{ex} = 300 nm) in different solvents.

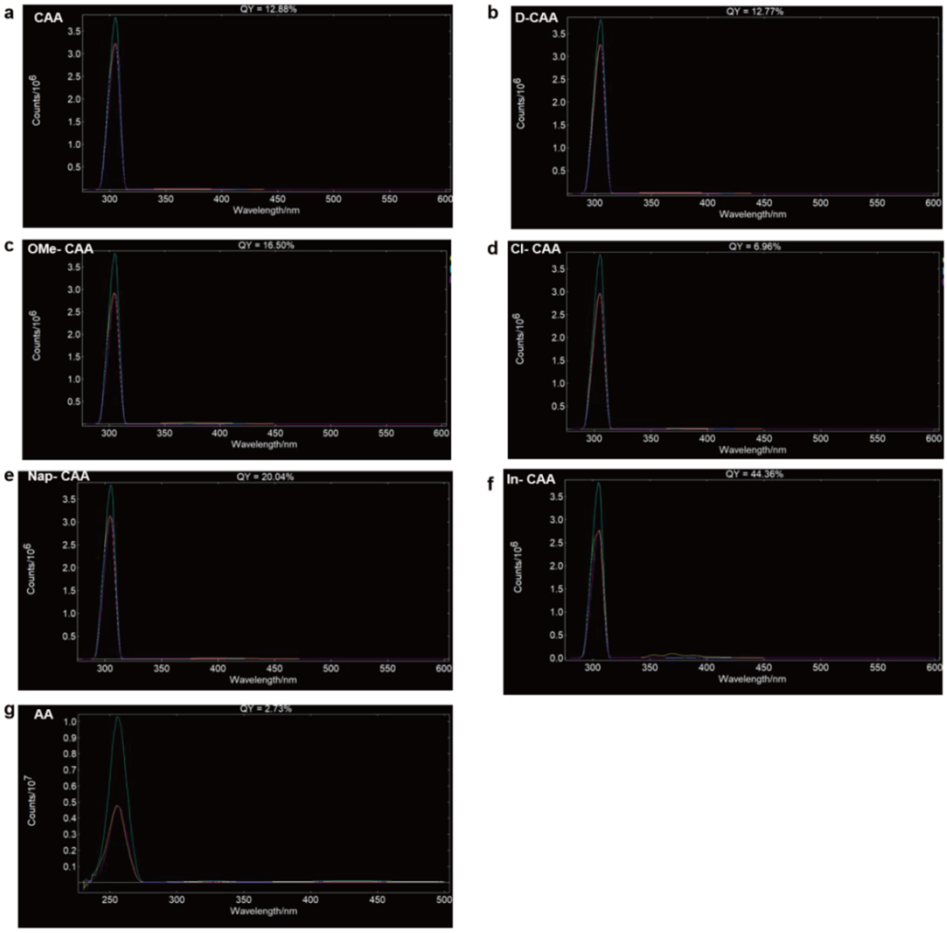

Fig. S22 Total quantum yields of CAA, D-CAA, OMe-CAA, Cl-CAA, In-CAA, Nap-CAA and AA in acetonitrile solution (λ_{ex} = 300 nm, C = 1.0×10^{-5} M).

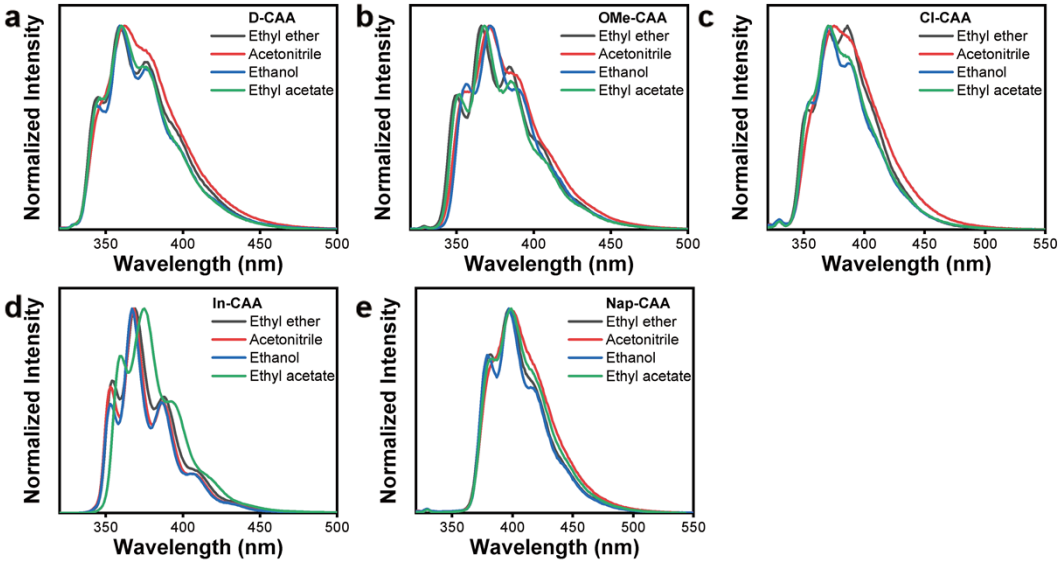

Fig. S23 Fluorescence spectra of D-CAA, OMe-CAA, Cl-CAA, In-CAA and Nap-CAA (C = 1.0×10^{-5} M, λ_{ex} = 300 nm) in different solvents.

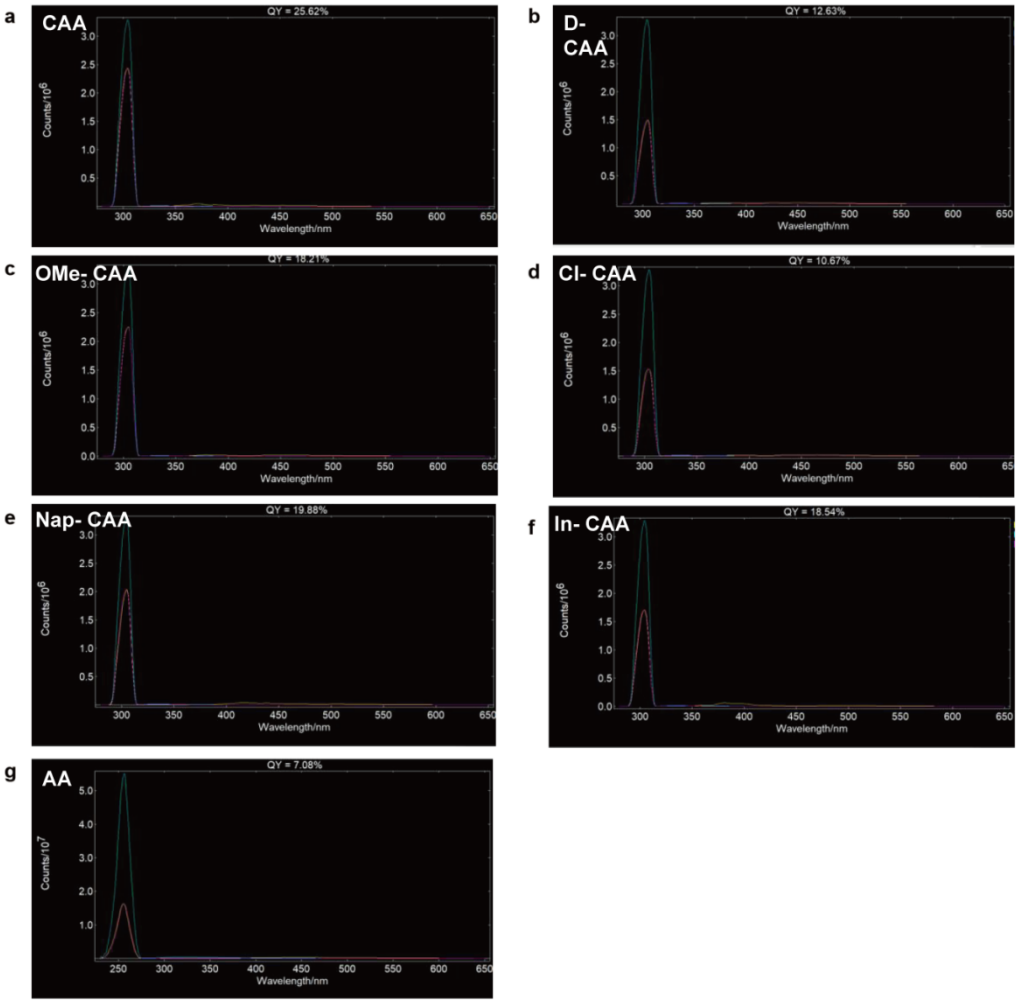

Fig. S24 Total quantum yields of CAA@PVA, D-CAA@PVA, OMe-CAA@PVA, Cl-CAA@PVA, Nap-CAA@PVA, In-CAA@PVA and AA@PVA at 0.3% ratio.

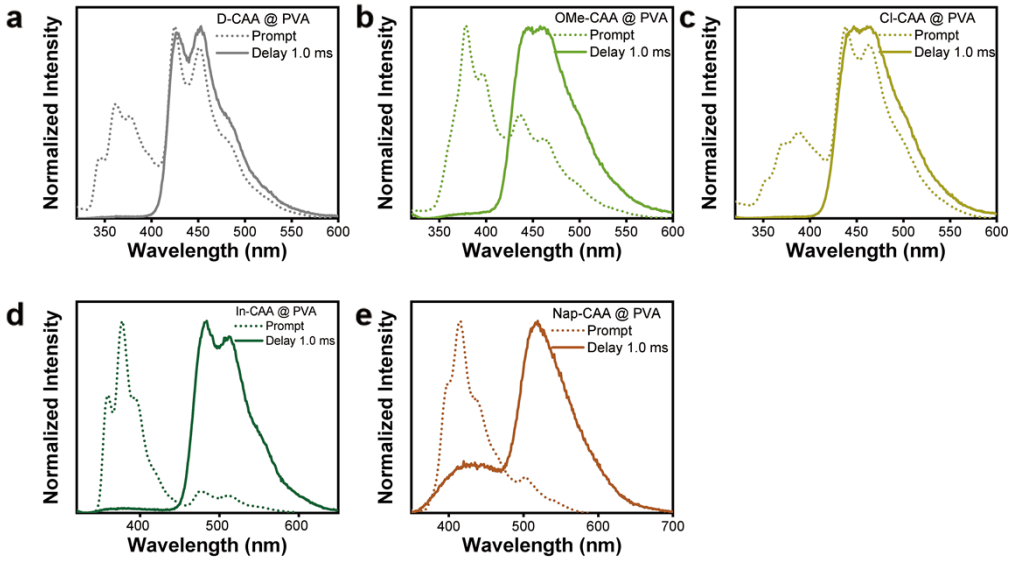

Fig. S25 Prompt and delayed emission spectra of D-CAA@PVA, OMe-CAA@PVA, Cl-CAA@PVA, In-CAA@PVA and Nap-CAA@PVA (λ_{ex} = 300 nm, delayed time = 1.0 ms).

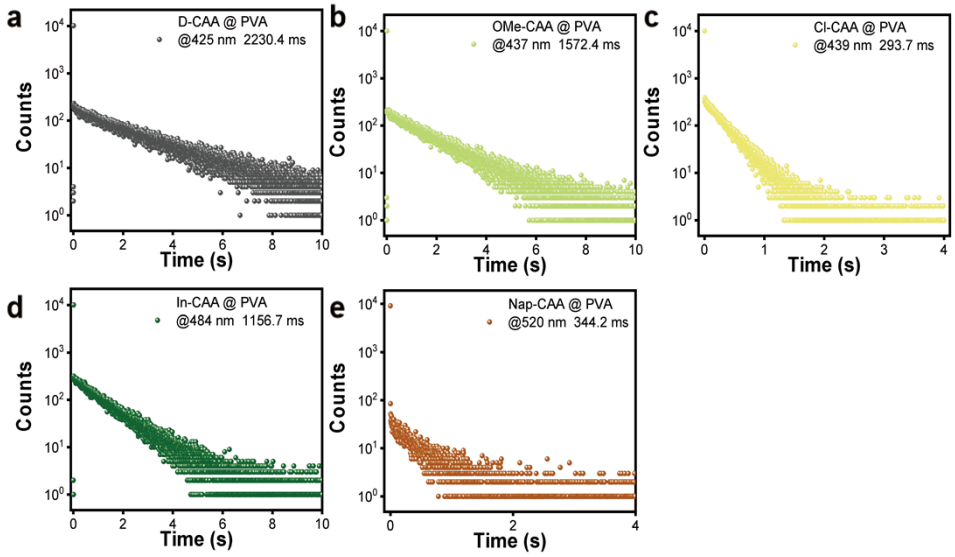

Fig. S26 Phosphorescence decay profiles of D-CAA, OMe-CAA, Cl-CAA, In-CAA and Nap-CAA in PVA at a ratio of 0.3%.

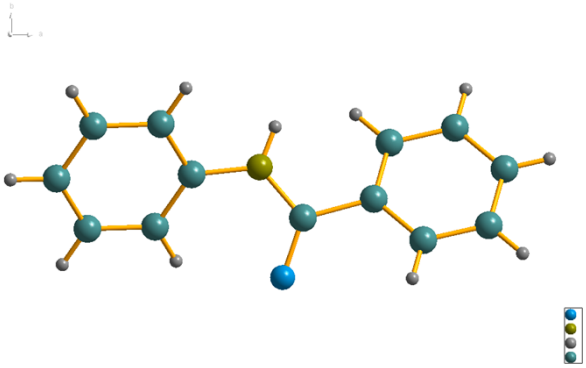

Fig. S27 Single-crystal X-Ray structure of AA

Table S9. Single-crystal X-Ray data of AA.

Empirical formula	C13 H11 N O
Formula weight	197.23
Temperature / K	180
Crystal system	monoclinic
Space group	C 2/c
a / Å	24.421(4)
b / Å	5.3378(9)
c / Å	7.8439(11)
α / °	90
β / °	107.445(13)
γ / °	90
Volume / Å^3	975.46(30)
Z	4
ρ_{calc}g / cm^3	1.343
μ / mm^{-1}	0.085
F(000)	416
Crystal size / mm^3	0.14*0.12*0.06
Radiation	MoKα (λ =0.71073)
2Θ range for data collection /°	1.748 to 24.988
Index ranges	28,6,8
Reflections collected	3383
Independent reflections	854
Data/restraints/parameters	854/0/72
Goodness-of-fit on F2	1.056
Final R indexes [I>=2σ (I)]	R1 = 0.0959, wR2 = 0.2178
Final R indexes [all data]	R1 = 0.1018, wR2 = 0.2203
Largest diff. peak/hole / e Å^{-3}	0.325/-0.300

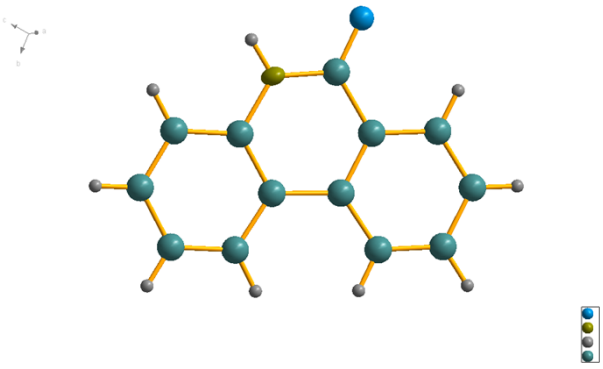

Fig. S28 Single-crystal X-Ray structure of CAA.

Table S10. Single-crystal X-Ray data of CAA.

Empirical formula	C13 H9 N O
Formula weight	195.21
Temperature / K	179.99
Crystal system	orthorhombic
Space group	P 21 21 21
a / Å	4.5969(3)
b / Å	12.4629(9)
c / Å	15.9326(12)
α / °	90
β / °	90
γ / °	90
Volume / Å^3	912.79(11)
Z	4
ρ_{calc}g / cm^3	1.421
μ / mm^{-1}	0.091
F(000)	408
Crystal size / mm^3	0.56*0.04*0.03
Radiation	MoKα (λ =0.71073)
2Θ range for data collection /°	2.557 to 29.397
Index ranges	3,9,20
Reflections collected	3822
Independent reflections	2104
Data/restraints/parameters	2104/0/136
Goodness-of-fit on F2	1.010
Final R indexes [I>=2σ (I)]	R1 = 0.0609, wR2 = 0.1468
Final R indexes [all data]	R1 = 0.0825, wR2 = 0.1573
Largest diff. peak/hole / e Å^{-3}	0.319/-0.324

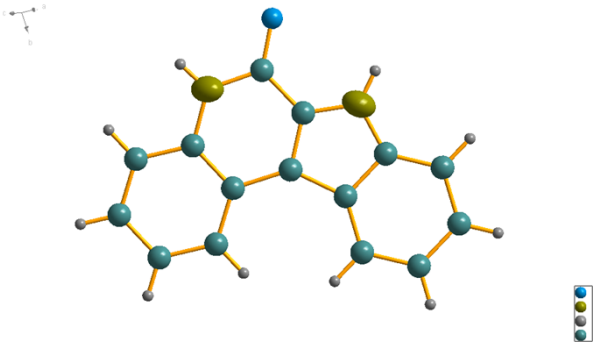

Fig. S29 Single-crystal X-Ray structure of In-CAA.

Table S11. Single-crystal X-Ray data of In-CAA.

Empirical formula	C15 H10 N2 O
Formula weight	234.25
Temperature / K	179.99
Crystal system	triclinic
Space group	P -1
a / Å	12.5592(5)
b / Å	12.7823(5)
c / Å	17.5673(6)
α / °	98.761(2)
β / °	96.476(2)
γ / °	119.427(3)
Volume / Å^3	1045.50(5)
Z	2
ρ_{calc}g / cm^3	1.167
μ / mm^{-1}	0.075
F(000)	976
Crystal size / mm^3	0.41*0.13*0.04
Radiation	MoKα (λ =0.71073)
2Θ range for data collection /°	1.672 to 25.027
Index ranges	14,15,20
Reflections collected	31232
Independent reflections	9395
Data/restraints/parameters	9395/85/678
Goodness-of-fit on F2	1.055
Final R indexes [I>=2σ (I)]	R1 = 0.0807, wR2 = 0.2152
Final R indexes [all data]	R1 = 0.1024, wR2 = 0.2291
Largest diff. peak/hole / e Å^{-3}	0.399/-0.317

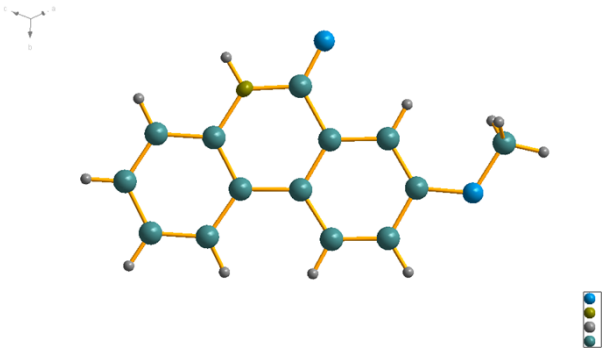

Fig. S30 Single-crystal X-Ray structure of OMe-CAA.

Table S12. Single-crystal X-Ray data of OMe-CAA.

Empirical formula	C14 H11 N O2
Formula weight	225.24
Temperature / K	180.00
Crystal system	monoclinic
Space group	P 21/n
a / Å	11.6308(5)
b / Å	5.5299(2)
c / Å	16.6438(6)
α / °	90
β / °	104.775(4)
γ / °	90
Volume / Å^3	1035.09(7)
Z	4
ρ_{calc}g / cm^3	1.445
μ / mm^{-1}	0.098
F(000)	472
Crystal size / mm^3	0.22*0.11*0.08
Radiation	MoKα (λ =0.71073)
2Θ range for data collection /°	2.460 to 29.388
Index ranges	13,6,22
Reflections collected	6405
Independent reflections	2591
Data/restraints/parameters	2591/0/155
Goodness-of-fit on F2	1.065
Final R indexes [I>=2σ (I)]	R1 = 0.0403, wR2 = 0.1161
Final R indexes [all data]	R1 = 0.0480, wR2 = 0.1222
Largest diff. peak/hole / e Å^{-3}	0.275/-0.266

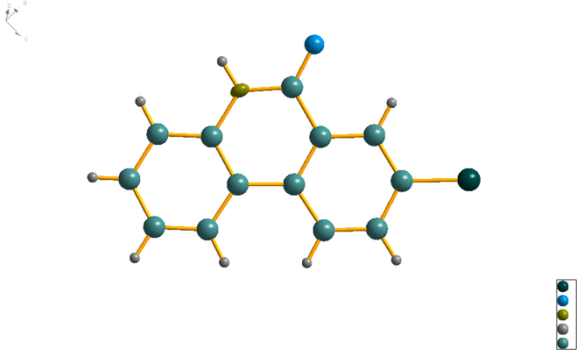

Fig. S31 Single-crystal X-Ray structure of Cl-CAA

Table S13. Single-crystal X-Ray data of Cl-CAA.

Empirical formula	C13 H8 Cl N O
Formula weight	229.65
Temperature / K	180.00
Crystal system	monoclinic
Space group	P 21/n
a / Å	12.7960(6)
b / Å	3.8255(2)
c / Å	20.1892(9)
α / °	90
β / °	97.742(4)
γ / °	90
Volume / Å^3	979.28(8)
Z	4
ρ_{calc}g / cm^3	1.558
μ / mm^{-1}	0.361
F(000)	472
Crystal size / mm^3	0.33*0.07*0.04
Radiation	MoKα (λ =0.71073)
2Θ range for data collection /°	2.036 to 29.445
Index ranges	14,5,27
Reflections collected	5684
Independent reflections	2414
Data/restraints/parameters	2414/0/145
Goodness-of-fit on F2	1.064
Final R indexes [I>=2σ (I)]	R1 = 0.0354, wR2 = 0.0978
Final R indexes [all data]	R1 = 0.0446, wR2 = 0.1037
Largest diff. peak/hole / e Å^{-3}	0.324/-0.253

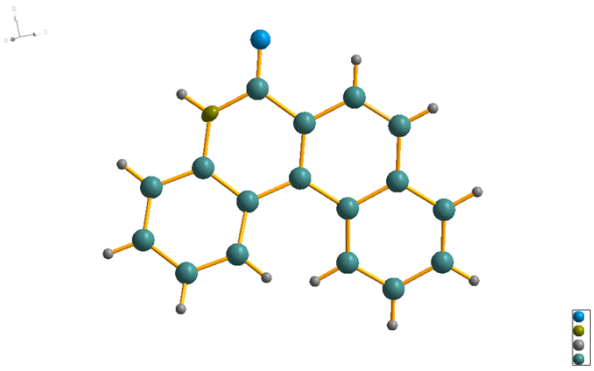

Fig. S32 Single-crystal X-Ray structure of Nap-CAA.

Table S14. Single-crystal X-Ray data of Nap-CAA.

Empirical formula	C17 H11 N O
Formula weight	245.27
Temperature / K	180.01
Crystal system	orthorhombic
Space group	P 21 21 21
a / Å	3.8342(2)
b / Å	14.7555(6)
c / Å	19.9746(9)
α / °	90
β / °	90
γ / °	90
Volume / Å^3	1130.07(9)
Z	4
ρ_{calc}g / cm^3	1.442
μ / mm^{-1}	0.090
F(000)	512
Crystal size / mm^3	0.31*0.08*0.07
Radiation	MoKα (λ =0.71073)
2Θ range for data collection /°	2.463 to 29.403
Index ranges	3,19,27
Reflections collected	4773
Independent reflections	2483
Data/restraints/parameters	2483/0/172
Goodness-of-fit on F2	1.063
Final R indexes [I>=2σ (I)]	R1 = 0.0356, wR2 = 0.0909
Final R indexes [all data]	R1 = 0.0401, wR2 = 0.0945
Largest diff. peak/hole / e Å^{-3}	0.218/-0.228

References

1. Y. Kuwata, M. Sonoda and S. Tanimori, *J. Heterocyclic. Chem*, 2016, **54**, 1645-1651.
2. K. Tanimoto, N. Nakagawa, K. Takeda, M. Kirihata and S. Tanimori, 2013, **54**, 3712-3714.
3. J. Guo, C. Wang, Q. He, X. Yang, X. Guo, B. Chen, C. Tung and L. Wu, *J. Photoch. Photobio. A.*, 2025, **460**, 116113.
4. C. Adamo and V. Barone, *J. Phys. D: Appl. Phys.*, 1999, **110**, 6158-6170.
5. F. Weigend and R. Ahlrichs, Balanced basis sets of split valence, *Phys Chem Chem Phys*, 2005, **7**, 3297-3305.
6. V. Marenich, J. Cramer and G. Truhlar, *J. Phys. Chem. B.* 2009, **113**, 6378-6396.
7. F. Neese, *Comput. Mol. Sci.*, 2011, **2**, 73-78.
8. W. Humphrey, A. Dalke and K. Schulten, *J. Mol. Graph. Model.* 1996, **14**, 33-88.